

# Inbreeding reduces long-term growth of Alpine ibex populations

Claudio Bozzuto <sup>1,5,6</sup>, Iris Biebach <sup>1,6</sup>, Stefanie Muff <sup>1,2</sup>, Anthony R. Ives <sup>3\*</sup> and Lukas F. Keller <sup>1,4\*</sup>

**Many studies document negative inbreeding effects on individuals, and conservation efforts to preserve rare species routinely employ strategies to reduce inbreeding. Despite this, there are few clear examples in nature of inbreeding decreasing the growth rates of populations, and the extent of population-level effects of inbreeding in the wild remains controversial. Here, we take advantage of a long-term dataset of 26 reintroduced Alpine ibex (*Capra ibex ibex*) populations spanning nearly 100 years to show that inbreeding substantially reduced per capita population growth rates, particularly for populations in harsher environments. Populations with high average inbreeding ( $F \approx 0.2$ ) had population growth rates reduced by 71% compared with populations with no inbreeding. Our results show that inbreeding can have long-term demographic consequences even when environmental variation is large and deleterious alleles may have been purged during bottlenecks. Thus, efforts to guard against inbreeding effects in populations of endangered species have not been misplaced.**

Inbreeding depression, the harmful effects of inbreeding on the fitness of individuals, is widespread among plants and animals, with recent genomic studies revealing an even greater impact on individual fitness than previously thought<sup>1</sup>. However, reduced fitness of individuals due to inbreeding does not necessarily lead to reduced population growth rates<sup>2–4</sup>, in the same way that natural selection need not impact population growth<sup>5</sup>. Instead, theory predicts that the degree to which inbreeding depression affects population growth will depend on the ecology and life history of a species<sup>3,6</sup>. For example, in species experiencing density-dependent population growth, even substantial inbreeding depression at the individual level need not translate into reduced population growth, because fitness reductions caused by inbreeding may be compensated by fitness gains caused by relaxed competition. Under such circumstances, inbred individuals may produce enough offspring to maintain population growth (soft selection<sup>7</sup>).

Collecting unequivocal evidence for population-level effects of inbreeding is difficult, because it requires many replicated populations that differ in levels of inbreeding to be monitored over many generations. Hence, the extent of population-level effects of inbreeding in the wild remains controversial<sup>7–9</sup>, and we currently lack an understanding of the magnitude of the consequences of inbreeding depression for long-term population growth in natural populations<sup>10</sup>. Here, we take advantage of a long-term dataset of 26 reintroduced Alpine ibex populations (Supplementary Figs. 1 and 2) spanning 23–96 years to show that inbreeding can reduce long-term population growth rates in the wild.

Alpine ibex were extirpated from the Alps by the end of the nineteenth century, with only a single population surviving in the Gran Paradiso region in northern Italy<sup>11</sup>. Starting in 1906, Alpine ibex were taken from Gran Paradiso, bred in Swiss zoos and then released back into their former habitat. These reintroductions are well documented<sup>12</sup>, with counts of the released individuals, subsequent time series of annual abundance counts and counts of the numbers of harvested animals (Supplementary Table 1). Genetic

data suggest little natural migration between populations after reintroductions ceased<sup>13</sup>, making the populations distinct replicates for the purpose of this study.

The ibex populations in our study experienced up to four reintroduction-associated bottlenecks<sup>13</sup>. The first bottleneck occurred when the Swiss breeding programme was initiated with ~88 individuals from Gran Paradiso<sup>11</sup>. First reintroductions into the wild with ibex from the Swiss breeding programme caused a second set of bottlenecks (founder population sizes: 18–78). The third set of bottlenecks took place when individuals from the first founder populations were used to found additional wild populations (founder population sizes: 9–137). Subsequent reintroductions sourced some founder individuals from populations that had already experienced three bottlenecks, thus causing a fourth bottleneck<sup>13</sup>. Genetically, the bottlenecks were twice as pronounced as expected from the number of released founders because, on average, only about half of the founders contributed genes to the following generations<sup>14</sup>.

These serial bottlenecks resulted in considerable genetic drift and inbreeding<sup>15</sup>. In this study, we use the term inbreeding to refer to the average identity by descent across individuals that accumulates under random mating in a population of finite size in concert with genetic drift<sup>16,17</sup>. We quantified this inbreeding using 37 microsatellite loci and population-specific  $F_{ST}$  estimates that measure the probability of identity by descent of pairs of alleles at a locus within populations relative to pairs of alleles from different populations<sup>18,19</sup>. Population-specific  $F_{ST}$  estimates were calculated for each population individually. Averaged across all populations, they yield the familiar global  $F_{ST}$  estimate<sup>19</sup>. There is no evidence for inbreeding due to non-random mating within Alpine ibex populations ( $F_{IS} \approx 0$ ); therefore, population-specific  $F_{ST}$  estimates quantify total inbreeding since the last common ancestral population<sup>18,20</sup> at the beginning of the reintroduction programme about 12.5 generations ago<sup>13</sup>. Population-specific  $F_{ST}$  does not suffer from the same lack of power as individual inbreeding coefficients estimated from limited molecular data<sup>10,15</sup>, because limited dispersal and population

<sup>1</sup>Department of Evolutionary Biology and Environmental Studies, University of Zurich, Zurich, Switzerland. <sup>2</sup>Department of Mathematical Sciences, Norwegian University of Science and Technology, Trondheim, Norway. <sup>3</sup>Department of Integrative Biology, University of Wisconsin-Madison, Madison, WI, USA. <sup>4</sup>Zoological Museum, University of Zurich, Zurich, Switzerland. <sup>5</sup>Present address: Wildlife Analysis GmbH, Zurich, Switzerland. <sup>6</sup>These authors contributed equally: Claudio Bozzuto, Iris Biebach. \*e-mail: [arives@wisc.edu](mailto:arives@wisc.edu); [lukas.keller@ieu.uzh.ch](mailto:lukas.keller@ieu.uzh.ch)

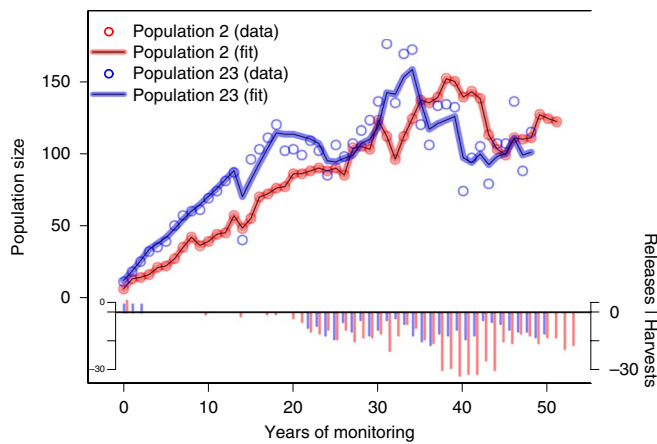


**Fig. 1 | Two representative Alpine ibex populations analyzed in this study.** Time series of annual abundance counts (dots), together with the nonlinear state-space model fits (lines), for the relatively inbred population 2 (red, with point estimates  $r_0 = 0.14$  and  $F_{ST} = 0.18$ ) and the relatively outbred population 23 (blue, with point estimates  $r_0 = 0.34$  and  $F_{ST} = 0.06$ ). Numbers of released ( $>0$ ) and harvested animals ( $<0$ ) are shown on separate x and y axes. Note the clear differences in population growth in the first 15–20 years, reflected in the corresponding differences in estimates of the per capita growth rates,  $r_0$ . Time series characteristics are summarized in Supplementary Table 1 and estimated model parameters are presented in Supplementary Table 2.

structure create identity disequilibrium and thus correlation in heterozygosity across loci<sup>21</sup>.

To estimate long-term population growth rates, we fitted a nonlinear state-space population model to each of the 26 populations, containing terms for the continuous rate of increase ( $r_0$ ), density dependence in population growth, the number of reintroduced as well as harvested individuals, environmental and demographic stochasticity, and sampling variability. Figure 1 shows two example populations and the fit of the state-space model to the data. To quantify the impact of inbreeding on population growth, we regressed  $r_0$  estimates against inbreeding and other covariates. Using a conventional regression approach would substantially underestimate the inbreeding effects, since inbreeding levels are known only with uncertainty, thus violating the important assumption of regressions that covariates are known exactly<sup>22</sup>. To obtain unbiased estimates of the effects of inbreeding on population growth, we incorporated the uncertainty in population-specific  $F_{ST}$  estimates using Bayesian heteroscedastic measurement-error models<sup>23</sup>. In addition, we explicitly accounted for uncertainties in estimates of  $r_0$ , and because larger values of  $r_0$  showed systematically larger variances (Supplementary Fig. 3a), we log-transformed  $r_0$  for all our regression models. In addition to inbreeding, the models included as covariates the year when the time series of a population began and climatic variables known to affect ibex populations<sup>12</sup> but averaged across the entire length of the time series to capture environmentally induced spatial variation in population growth: mean daily summer and winter temperatures, mean daily summer and winter precipitation, and winter snow cover. Due to the Bayesian nature of the analysis, model selection was guided by deviance information criterion (DIC) minimization.

## Results

The best-fitting model (Table 1), which captured 79% of the variation in log-transformed continuous rates of increase among the 26 populations (Supplementary Tables 3 and 4), revealed evidence for a negative effect of inbreeding on population growth rates in conjunction with climatic variables (Fig. 2). According to the model, a population-specific  $F_{ST}$  of 0.21 (the maximum inbreeding observed

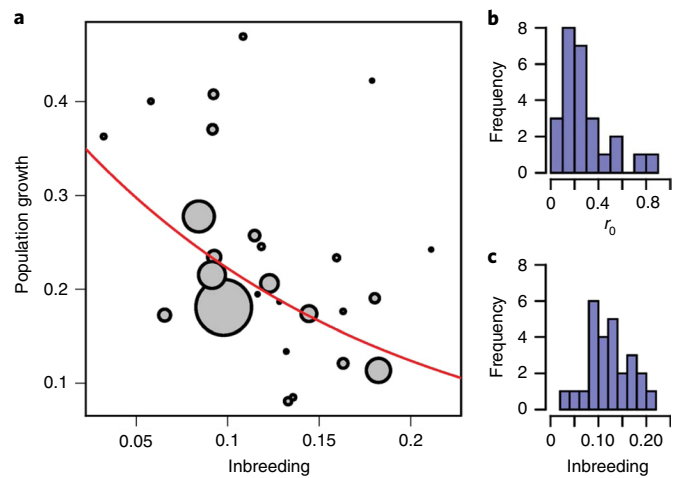


**Fig. 2 | Visualization of the effect of inbreeding on population growth.** **a**, Main effect of inbreeding, measured by population-specific  $F_{ST}$  ('Inbreeding', x axis), on the continuous rate of increase,  $r_0$  ('Population growth', y axis), among 26 populations of Alpine ibex. Values of  $r_0$  were adjusted for all covariates in the model except for the main effects of  $F_{ST}$ . The area of each point is inversely proportional to the error variances in the estimates of  $r_0$  from the time series, which are used in the error model to down-weight observations with large uncertainty. **b, c**, The absolute frequency distribution of estimates of  $r_0$  (**b**) and  $F_{ST}$  (**c**) for the 26 Alpine ibex populations.

in this study) reduced the expected  $r_0$  by 71% with respect to a hypothetical population with zero inbreeding, while a population-specific  $F_{ST}$  of 0.03 (the observed minimum) led to only a 17% reduction. As expected from measurement-error theory, regressions that did not account for the uncertainty in estimates of inbreeding yielded substantially downwardly biased estimates of the impacts of inbreeding (Supplementary Table 3).

Environmental factors represented by the averaged climate variables had strong effects on population growth rates, and the magnitude of inbreeding effects depended on these environmental conditions (Table 1): inbreeding effects on population growth rates were absent in areas with low summer precipitation, but were increasingly pronounced in areas with wetter summers (Fig. 3). This may represent a direct effect of summer precipitation through adverse effects on neonatal mortality or body growth<sup>12</sup>. However, given that the climate variables represent averages across the entire time series period, the effect may have different, indirect causes that we cannot identify since our study was not designed to isolate the causes of environmental variation in  $r_0$ . Whatever the cause, our findings support theoretical predictions that ecological processes can modify the population-level effects of inbreeding<sup>3</sup>, and they mirror many studies at the individual level that show inbreeding depression can vary with environmental conditions<sup>24</sup>.

We have shown that inbreeding reduces long-term population growth rates. However, population growth rates in turn can affect levels of inbreeding: low population growth rates will keep populations small, which increases genetic drift and hence the amount of inbreeding<sup>15,25</sup>. Could the observed effect of inbreeding on population growth be confounded by an effect of population growth on inbreeding? Theory does not predict a straightforward effect of population growth rate on inbreeding. Instead, the expected inbreeding in a randomly mating population is determined by the harmonic mean population size<sup>26</sup>, which in turn is a nonlinear function of population growth rate and the founding population size (equation (A3) in Beaumont<sup>27</sup>). In our data,  $r_0$  and harmonic mean population sizes were not correlated ( $r = -0.07$ , 95% confidence interval

**Table 1 | Results of the regression analysis**

Model	DIC	$\hat{\beta}_F$	$\hat{\beta}_{\text{year}}$	$\hat{\beta}_{\text{pw}}$	$\hat{\beta}_{\text{ps}}$	$\hat{\beta}_{\text{year} \times \text{ps}}$	$\hat{\beta}_{F \times \text{ps}}$
1	-6.61	-5.85 [-13.02, 0.84]	0.0223 [0.0111, 0.0343]	0.610 [0.457, 0.770]	-0.510 [-0.713, -0.325]	-0.0218 [-0.0345, -0.0098]	-4.22 [-8.57, -0.71]
2	0.261	-8.56 [-15.61, -1.54]	0.0240 [0.0116, 0.0367]	0.622 [0.453, 0.792]	-0.486 [-0.673, -0.300]	-0.0213 [-0.0341, -0.0087]	

Parameter estimates (posterior means and 95% credible intervals) for the effects of inbreeding ( $\hat{\beta}_F$ ), the year when the time series began ( $\hat{\beta}_{\text{year}}$ ), mean precipitation in winter ( $\hat{\beta}_{\text{pw}}$ ), mean precipitation in summer ( $\hat{\beta}_{\text{ps}}$ ) and two interaction terms ( $\hat{\beta}_{\text{year} \times \text{ps}}$  and  $\hat{\beta}_{F \times \text{ps}}$ ) on the log-transformed continuous population growth rate,  $r_0$ ;  $F$  is short for  $F_{ST}$  (sub-indices). Model 1 includes the interaction between inbreeding and summer precipitation, whereas model 2 does not.

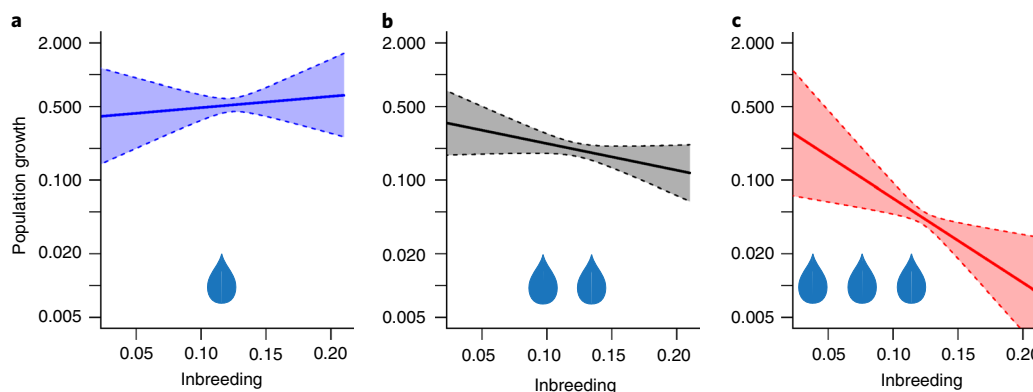


**Fig. 3 | Visualization of the estimated interaction effects of inbreeding and summer precipitation on population growth.** **a–c**, Minimal (**a**), mean (**b**) and maximal (**c**) values of summer precipitation (see Supplementary Table 3). Increased summer precipitation reduced population growth rates, implying that inbreeding effects on population growth rates were more pronounced in harsher environments. The shadowed areas represent the 95% credible ranges. Note the logarithmic scale (but  $r_0$  values untransformed) of the y axis when comparing Fig. 3 to Fig. 2a; as for Fig. 2a, the axis labels ‘Inbreeding’ and ‘Population growth’ refer to  $F_{ST}$  and  $r_0$ , respectively.

(CI):  $-0.44$  to  $0.33$ ,  $P=0.74$ ,  $N=26$ ; rearranging equation (A3) in Beaumont<sup>27</sup> to obtain a linear relationship), and adding harmonic mean population sizes to our regression models for  $r_0$  did not affect the overall conclusions (Supplementary Tables 1, 4 and 5). Thus, we found no evidence that variation in  $r_0$  among the populations in our dataset generated differences in inbreeding. Instead, variation in founder group size, admixture of the founder groups and carrying capacity appear to be the major sources of variation in inbreeding that arose among ibex populations since the beginning of the reintroduction programme<sup>14,15</sup>.

## Discussion

Our results support the emerging view that genetic processes can substantially affect long-term population growth, even in populations that may have purged deleterious recessive alleles during successive bottlenecks<sup>28,29</sup>. Our study design did not allow the detection of purging and so we can only speculate about this in Alpine ibex. Some purging may have occurred, as in some invasive species<sup>28</sup>, because conditions promoting decreases in population growth rates through inbreeding (that is, hard selection) also lead to purging<sup>6</sup>. However, the efficiency of purging depends on population size, and the relatively small bottleneck sizes of the Alpine ibex populations (with mean number of founding chromosomes of 42)<sup>14</sup> imply that purging would mostly remove strongly deleterious mutations<sup>29,30</sup>. The more weakly deleterious alleles may have drifted to fixation during the bottlenecks, creating drift load<sup>31</sup>, and those that were not fixed may be being purged now that population sizes have increased<sup>29</sup>. The combination of drift load and limited purging probably explains the substantial inbreeding effects in reintroduced Alpine ibex populations. Thus, genetic rescue with

increased population growth may result if ibex were translocated among populations<sup>1,32</sup>.

The population time series we analysed included periods of rapid growth and substantial declines, and show the impact of density dependence (Fig. 1). Yet the inbreeding effects were strong enough to overcome density-dependent compensation and reduce the growth of the reintroduced populations. One factor that may contribute to the strong demographic consequences of inbreeding in Alpine ibex is the relatively weak density dependence in many populations (Supplementary Table 2). Weak density dependence suggests that Alpine ibex do not compete strongly for limited resources. This leads to hard selection and, hence, reduced population growth because deaths due to inbreeding do not substantially relax the already low competition<sup>2,3</sup>. Thus, the relatively weak density dependence may have contributed to the observed demographic consequences of inbreeding in Alpine ibex.

Our results indicate that inbreeding can substantially lower long-term population growth even when deleterious alleles may have been purged during bottlenecks<sup>28</sup> and when populations are reintroduced into habitats to which they are adapted<sup>24</sup>. In line with theoretical predictions, we found that ecological conditions modify the extent to which inbreeding affects population growth, but they are unlikely to mask them completely<sup>3</sup>. Thus, when ecological conditions produce hard selection (for example, when density dependence is relatively weak, as in the case of most populations of conservation concern), inbreeding depression at the individual level can lead to large reductions in population growth. Ultimately, these effects can lead to increased extinction rates at the population and species level<sup>33–35</sup>.

As we have shown, detecting population-level effects of inbreeding requires an exceptional dataset, with many populations that

differ in inbreeding and enough environmental data to factor out other causes of reduced population growth rates. Even with the exceptional Alpine ibex data, detecting population-level inbreeding effects was a statistical challenge. Thus, it is not surprising that, despite the many examples of individual-level inbreeding effects in nature, population-level effects on the dynamics of wild populations have rarely been documented unambiguously.

## Methods

**Study populations and population-related data.** Alpine ibex populations in Switzerland have been monitored closely since their reintroductions, with yearly abundance counts usually conducted in spring<sup>36</sup>. At this time of year, ibex are found in fairly restricted areas below the snow line and just above timberline<sup>37</sup> and are therefore easier to count than most other ungulates. Hence, Saether et al.<sup>38</sup> found the error in population censuses to be small (with median coefficient of variation across 28 ibex populations of 5.1%). In addition to abundance count data, we had time series for: (1) the number of released animals, (2) the number of harvested animals for all but a single non-hunted population (number 22), and (3) the number of animals that were removed for translocations. Initial releases were performed at the end of winter. Harvest of ibex populations started in 1977, when many populations had grown to high densities. In some populations ibex were removed for translocation to other populations. In our study, these ibex were considered to be harvested and were added to the count of harvested animals in that year. This explains why the first year for harvesting can be before 1977 (Supplementary Table 1, column 'Hunting'). We analysed data of 26 Alpine ibex populations, with time series ranging from 23 to 96 years (Supplementary Table 1). For this study we added genetic data from three populations (numbers 24, 25 and 26) to 23 populations that had previously been analysed genetically<sup>13</sup>.

**Inference of inbreeding level.** An average of 36.9 (range 17–102) individuals from each of the 26 populations were genotyped at 37 neutral microsatellite loci as detailed in Biebach et al.<sup>13</sup>. Most inbreeding in the reintroduced Alpine ibex populations accumulated in concert with genetic drift during founder events and during the time when population sizes were low following reintroduction<sup>15</sup>. We quantified the inbreeding that arose following the start of the reintroduction programme more than 100 years ago using marker-based population-specific  $F_{ST}$ <sup>18,19</sup>. Population-specific  $F_{ST}$  of population  $i$  is defined as  $F_{ST,i} = (\theta_i - \theta_A) / (1 - \theta_A)$ , where  $\theta_i$  is the probability of a gene being identical by descent (IBD) within population  $i$ , and  $\theta_A$  is the probability of a gene being IBD between all populations<sup>18</sup>. In line with theory, simulations have shown that  $F_{ST}$  explains a substantial part of the effects of deleterious mutations on population fitness<sup>39</sup>, making  $F_{ST}$  a suitable measure of average population inbreeding for this study.

We used a Bayesian framework in a modified version of 2MOD<sup>40</sup> to estimate population-specific  $F_{ST}$  for 42 ibex populations<sup>15</sup>. For the present study, we used the results of 26 populations for which we also had abundance data. All parameters were given uninformative flat prior distributions. We used the non-equilibrium drift model in 2MOD that estimates inbreeding relative to the last common ancestral population. The model assumes that the reciprocal of the mutation rate is much longer than the divergence time<sup>40</sup>, which is a reasonable assumption for the reintroduced ibex populations since they were founded no more than 12.5 generations ago. In our case, the ancestral reference population is the Gran Paradiso population in Italy, the single remaining population of Alpine ibex before animals were transferred to found the zoo populations that were the source for the first reintroductions. Thus, the estimated inbreeding coefficient measures the accumulated inbreeding from the start of the reintroduction programme in 1906. The ancestral reference population used here differs from that used in previous studies of inbreeding in Alpine ibex<sup>15</sup>, and therefore results are not directly comparable.

The observed degree of inbreeding will depend on the composition of the founder population and the harmonic mean population size after founding (inbreeding  $N_i$ ). The length of the time series is not expected to influence the inbreeding coefficient ( $r = -0.27$ , 95% CI:  $-0.60$  to  $0.13$ ,  $P = 0.18$ ,  $N = 26$ ) because harmonic mean population size is mainly determined by the small population sizes early in the development of the population<sup>15</sup>. As expected, given that inbreeding measures IBD and homozygosity measures identity-in-state, mean observed homozygosity and population-specific  $F_{ST}$  were only moderately correlated ( $r = 0.55$ , 95% CI:  $0.21$  to  $0.77$ ,  $P = 0.003$ ,  $N = 26$ ) across the 26 populations.  $F_{ST}$  estimates are not only affected by statistical sampling variance, but also by genetic sampling variance caused by genetic drift<sup>20</sup>; therefore, their credible intervals are substantial even when based on three dozen loci (Supplementary Table 6). We estimated mean, variance and 95% credible intervals of population-specific  $F_{ST}$  for each population from 450,000 iterations with the R-package STATS<sup>41</sup>.

Next-generation sequencing methods offer alternative measures of individual inbreeding coefficients<sup>40</sup>. In our study system, estimates of runs of homozygosity (total length of runs of homozygosity > 5 Mb, see also Supplementary information) based on 31,580 single-nucleotide polymorphisms obtained with RAD-sequencing<sup>42</sup> of 99 ibex averaged across each of ten populations yielded very

similar estimates of population-level inbreeding ( $r = 0.82$ , 95% CI:  $0.39$  to  $0.96$ ,  $P = 0.004$ ,  $N = 10$ , Supplementary Table 7). Thus, next-generation sequencing data confirm the population-level estimates of inbreeding obtained with microsatellites in this study.

**Population dynamics: model description.** In constructing the population dynamics model, we followed the dynamically important steps of a population through a year. We started the cycle with population size in spring, coinciding with the time when counts were made. We then added reproduction in summer. In autumn, hunting of adults takes place before the December–January rut<sup>43</sup>. Thus, only the proportion not killed was retained in the model. Winter is the season when most natural mortality occurs; thus, we included density-dependent mortality. Finally, we added the reintroduced animals.

Combining these components of ibex population dynamics leads to the discrete-time dynamical equation

$$N_t = N_{t-1} e^{r_0} \left(1 - \frac{H_{t-1}}{N_{t-1}}\right) f(N_{t-1} - H_{t-1}) \times \left(1 + \frac{R_{t-1}}{e^{b_0(N_{t-1} - H_{t-1})} f(N_{t-1} - H_{t-1})}\right) e^{\epsilon_t} e^{\phi_t} \quad (1)$$

Here,  $N_t$  is the 'true' (unobserved) population abundance before reproduction in spring in year  $t$ ;  $r_0$  is the density-independent (intrinsic) continuous rate of increase;  $H_t$  is the number of adult animals harvested in year  $t$ ;  $f(N_{t-1} - H_{t-1})$  is a function giving density-dependent survival that depends on the number of individuals in the population, excluding kids born that year and harvested individuals;  $R_t$  is the number of individuals added to the population following overwintering survival;  $\epsilon_t$  is a random variable giving the effect of environmental variation on population growth and  $\phi_t$  is a random variable for demographic stochasticity. We assumed that the function  $f$  is a Gompertz equation, so that  $f(N_{t-1} - H_{t-1}) = \exp(b \log(N_{t-1} - H_{t-1}))$ , where the strength of density dependence  $b \leq 0$ , and smaller parameter values imply stronger density dependence. Taking  $x_t = \log(N_t)$  and rearranging gives the model

$$x_t = r_0 + \log\left((e^{x_{t-1}} - H_{t-1})^{(1+b)} + e^{-r_0} R_{t-1}\right) + \epsilon_t + \phi_t \quad (2)$$

The year-to-year fluctuations in 'true' population abundances, referred to as process variation in state-space models, are assumed to have two components: demographic stochasticity ( $\phi_t$ ) that decreases with increasing population size and environmental variability ( $\epsilon_t$ ). Environmental variation is assumed to have variance independent of the mean (on a log scale), and thus we take  $\epsilon_t$  as independent draws from a Gaussian random variable with mean 0 and variance  $\sigma_{\text{env}}^2$  (of the environmental stochasticity). In contrast, demographic stochasticity depends on the mean log population size. Assuming that demographic stochasticity follows a Poisson process, the resulting variation can be approximated by treating  $\phi_t$  as a Gaussian random variable with mean 0 and variance  $\log(\sigma_{\text{dem}}^2 e^{-x_{t-1}} + 1)$ , where  $\sigma_{\text{dem}}^2$  is the density-independent variance component of demographic stochasticity.

Since the 'true' population abundance  $N_t$  cannot be observed directly, our model takes a state-space form to account for the observation process. We assume that population counts follow a binomial process, and therefore observation error ( $\sigma_{\text{obs}}^2$ ) can be approximated as a Gaussian random variable  $\eta_t$  with mean 0 and variance  $\log(\sigma_{\text{obs}}^2 e^{-x_{t-1}} + 1)$ , where  $\sigma_{\text{obs}}^2$  is the density-independent variance component of the observation error. A full statement of the state-space model is

$$x_t = r_0 + \log\left((e^{x_{t-1}} - H_{t-1})^{(1+b)} + e^{-r_0} R_{t-1}\right) + \epsilon_t + \phi_t \quad (3a)$$

$$y_t = x_t + \eta_t \quad (3b)$$

$$\epsilon_t \sim N(0, \sigma_{\text{env}}^2) \quad (3c)$$

$$\phi_t \sim N(0, \log(\sigma_{\text{dem}}^2 e^{-x_{t-1}} + 1)) \quad (3d)$$

$$\eta_t \sim N(0, \log(\sigma_{\text{obs}}^2 e^{-x_{t-1}} + 1)) \quad (3e)$$

where  $y_t$  is the log-transformed observed number of individuals in the population in year  $t$ . Equations (3a) and (3b) are referred to as the process and observation equations, respectively, of the state-space model.

**Population dynamics: model fitting to data.** The model is nonlinear and in state-space form (equations 3a–e), and therefore we used an extended Kalman filter to calculate likelihoods and obtain the maximum likelihood parameter estimates<sup>44</sup>, using a procedure similar to Schooler et al.<sup>45</sup>; see also Supplementary information. Time series for several Alpine ibex populations have been analysed previously by Saether et al.<sup>38</sup> using a state-space model, although in a Bayesian context. In contrast to our study, Saether et al. did not include the release periods

in their analyses. We included release periods because they span a considerable number of years of early population growth (Supplementary Table 1) when density dependence was still low, and they therefore contain valuable information for estimating  $r_0$ . To prepare the time series for the extended Kalman filter analysis, for each population we (1) discarded years before the first available census count, (2) substituted subsequent counts of zero animals with 0.01 times the lowest non-zero census count and (3) substituted missing values with zero in the covariate time series of harvested and released animals.

We estimated simultaneously the five parameters  $r_0$ ,  $b$ ,  $\sigma_{\text{env}}^2$ ,  $\sigma_{\text{dem}}^2$  and  $\sigma_{\text{obs}}^2$ . Further, because the initial population sizes were small and therefore prone to observation error, we treated the first point in each time series,  $x_0$ , as an additional parameter to be estimated<sup>46</sup>.

We used simulated annealing to find optimal starting parameter values for the maximization routine and then refined the results using the Nelder–Mead simplex method<sup>47</sup>. Although it is theoretically possible to distinguish environmental, demographic and observation variation solely from time series data, in practice this is often impossible due to small sample sizes and the similarity of effects of different sources of variability on the observed time series. Therefore, the estimated values of  $\sigma_{\text{env}}^2$ ,  $\sigma_{\text{dem}}^2$  and  $\sigma_{\text{obs}}^2$  are sometimes zero (Supplementary Table 2), even though in reality they will not be. These zero estimates, however, will have very little effect on the estimates of  $r_0$ , the main target of the analyses.

To quantify the uncertainty in the point estimates of  $r_0$ , we calculated 95% confidence intervals using profile likelihoods<sup>48</sup>. Because the 95% confidence intervals around  $r_0$  were an important ingredient of the final regression analysis, we checked whether this uncertainty was significantly correlated to time series length or to the number of missing values (Supplementary Table 1). We found no significant correlation between  $1/\hat{\sigma}_{\log(r_0)}^2$  and time series length ( $r=0.01$ , 95% CI:  $-0.38$  to  $0.39$ ,  $P=0.97$ ,  $N=26$ ) or the number of missing data ( $r=-0.06$ , 95% CI:  $-0.44$  to  $0.33$ ,  $P=0.76$ ,  $N=26$ ).

**Regression analysis: model description.** We log-transformed  $r_0$  for the regression to account for three aspects of the estimates of  $r_0$ : (1) the uncertainty in estimates of  $r_0$  increased with the point estimate (Supplementary Fig. 3a), (2) most of the confidence intervals around single  $r_0$  estimates were right-skewed, and (3) the distribution of  $r_0$  point estimates was right-skewed (see also Supplementary Fig. 3b). Log-transforming  $r_0$  resolved all of these issues.

The regression models included as covariates the population-specific  $F_{\text{ST}}$ , five climate variables, and the year when the time series of a population began (Supplementary Table 1, column ‘Period’). We included the year when the time series began to account for possible changes in the suitability of habitats as reintroductions progressed. The climate variables were included because studies have shown effects of weather conditions on Alpine ibex population growth<sup>12</sup>. We obtained relevant data from the Swiss Federal Office of Meteorology and Climatology MeteoSwiss. All relevant weather stations for this study are located in a population’s habitat or in the immediate vicinity. From ecological knowledge of ibex, we split the year into summer (May–October) and winter (November–April). For each population we calculated one mean spanning the respective time series period for the following weather measures (Supplementary Table 8): daily mean air temperature in summer (ts) and winter (tw) (both in degrees Celsius), daily total precipitation in summer (ps) and winter (pw) (both in millimetres), and daily total snow cover in winter (sw) (in centimetres). Not all weather stations were recording data when the populations in this study were reintroduced. Thus, for some populations the climatic variables were calculated over a shorter time period than that for which we had time series data (Supplementary Table 1). These climate variables, averaged across the entire length of the time series, are a measure of the climate zone a population inhabits and are used to account for environmentally induced spatial variation in growth rates among populations. The effects captured by these averaged climate variables include indirect effects of variables that may covary with climate zone, such as spatial variation in food quality or quantity. The climate variables cannot, therefore, be interpreted in the same way that they have been in previous within-population studies<sup>12,38</sup>.

All covariates were centred by subtracting their respective mean value. Due to the log-transformation of  $r_0$ , variances were transformed by the delta rule for variance transformations:  $\hat{\sigma}_{\log(r_0)}^2 = \hat{\sigma}_0^2/r_0^2$  (Supplementary Fig. 3b). To account for the population-dependent (heteroscedastic) error in  $\log(r_0)$ , a random effects term with a population-specific variance, denoted as  $\delta_y$ , was added to the linear regression model.

Importantly, not only the response  $\log(r_0)$ , but also the covariate of interest,  $F_{\text{ST}}$ , has been estimated with uncertainty, that is, with measurement error. It is, however, a fundamental assumption of regression models that covariates have been precisely measured, and a violation of this assumption may lead to biased estimates of the regression coefficients<sup>22,49</sup>. Here, population-specific estimates of the uncertainty in the  $F_{\text{ST}}$  point estimates were available (see Inference of inbreeding level), and therefore we properly accounted for it by explicitly formulating an error model for this covariate. Note that measurement errors in covariates correlated with inbreeding could also bias the estimates of the inbreeding effects<sup>49</sup>, but because inbreeding was not substantially correlated with other covariates in the regression model (all  $r \leq 0.27$ ), we modelled only measurement error in inbreeding. We formulated a Bayesian hierarchical measurement-error model following the description in Muff et al.<sup>23</sup>, where the first level is the Gaussian regression model

relating population growth to the true covariates (equation (4a)), the second level is the classical Gaussian error model for the observed  $F_{\text{ST}}$  that accounts for unequal variances (heteroscedasticity; equation (4b)) and the third level is an independent Gaussian exposure model for the true but unobserved predictor  $F_{\text{ST}}$  (equation (4c)):

$$\log(r_0) = \beta_0 \mathbf{1} + \beta_F \mathbf{F}_{\text{true}} + \mathbf{Z}' \beta_z + \delta_y + \epsilon_y, \quad \epsilon_y \sim N(0, \sigma_y^2 \mathbf{I}), \quad (4a)$$

$$\delta_y \sim N(0, \mathbf{D}_y)$$

$$\mathbf{F}_{\text{ST}} = \mathbf{F}_{\text{true}} + \mathbf{u}, \quad \mathbf{u} \sim N(0, \mathbf{D}_u) \quad (4b)$$

$$\mathbf{F}_{\text{true}} = \boldsymbol{\mu}_0 + \boldsymbol{\epsilon}_{\text{Ftrue}}, \quad \boldsymbol{\epsilon}_{\text{Ftrue}} \sim N(0, \sigma_{\text{Ftrue}}^2 \mathbf{I}) \quad (4c)$$

Bold-face notation indicates vectors or matrices. The vector  $\mathbf{F}_{\text{true}}$  denotes the correct but unobserved inbreeding values,  $\mathbf{Z}$  is the matrix that contains the additional covariates as columns and  $\mathbf{Z}'$  is its transpose, and  $\beta_0$ ,  $\beta_F$  and  $\beta_z$  represent the intercept, slope coefficient of  $\mathbf{F}_{\text{true}}$ , and the vector of slope coefficients of  $\mathbf{Z}$ , respectively. The random term  $\delta_y$  accounts for the error in the observed  $\log(r_0)$  values.  $\mathbf{F}_{\text{ST}}$  is the vector of the estimated levels of inbreeding and  $\mathbf{u}$  is the error vector from the measurement-error model. Classical covariate measurement-error models require assigning a distribution to the predictor variable that is measured with error<sup>22</sup>, and we selected a Gaussian distribution (equation (4c)) with mean  $\boldsymbol{\mu}_0 = \mathbf{0}$  to match the observed (centred) distribution of  $F_{\text{ST}}$  scores (Fig. 2).

The variances  $\sigma_y^2$  and  $\sigma_{\text{Ftrue}}^2$  are the residual variance of the regression and the variance of  $\mathbf{F}_{\text{true}}$ , the entries in the diagonal matrices  $\mathbf{D}_y$  and  $\mathbf{D}_u$  account for population-specific (heteroscedastic) uncertainties in the regression and error models, respectively: the entries in the former are equal to the estimated error variances  $\hat{\sigma}_{\log(r_0)}^2$ , while the entries in the latter are equal to the estimated error variances  $\hat{\sigma}_{\text{FST}}^2$  for the individual populations, and thus these properly account for uncertainty in the  $\log(r_0)$  and  $F_{\text{ST}}$  estimates in each population, respectively. Matrix  $\mathbf{I}$  is the identity matrix, and  $\mathbf{1}$  is a vector of ones, both of appropriate dimension.

It is straightforward to incorporate prior knowledge into such a Bayesian hierarchical model, and in particular prior uncertainty given by the variance estimates. To estimate the posterior marginal distributions, we used a fast and accurate alternative to Markov chain Monte Carlo sampling, namely integrated nested Laplace approximations (INLA)<sup>50</sup>. INLA is suitable for inference on latent Gaussian models, which are a subset of hierarchical models and compatible with our model<sup>23</sup>.

We closely followed the procedure described in Muff et al.<sup>23</sup> to assign priors according to expert/prior knowledge. We used independent  $N(0, 10^4)$  priors for all  $\beta$ -coefficients, and inverse Gamma distributions for the variances:  $\sigma_y^2 \approx \text{IG}(1, 0.02)$  and  $\sigma_{\text{Ftrue}}^2 \approx \text{IG}(1.9, 0.001)$ . The  $\sigma_y^2$  prior differed from Muff et al.<sup>23</sup> because the log-transformed version of the response variable was used. Finally, the  $\mathbf{D}_y$  and  $\mathbf{D}_u$  entries were assumed to be known and are thus fixed.

**Regression analysis: model selection and parameter estimates.** Model selection was guided by minimization of the DIC<sup>51</sup>, where the main effect of interest,  $\beta_F$ , was always retained in the model. To illustrate the bias that would result if the uncertainty in the point estimates of population-specific  $F_{\text{ST}}$  were ignored, we also fitted the model with lowest DIC (termed ‘model 1’, Table 1) with a standard least squares approach using weighted regression with mean standardized weights proportional to  $1/\hat{\sigma}_{\log(r_0)}^2$ , but ignoring covariate error in inbreeding values (Supplementary Table 3, model 1(LS)). Further, we also retained a model that was identical to model 1, but that did not contain the interaction term ‘ $F_{\text{ST}} \times \text{ps}$ ’ (Table 1, model 2). Here, too, we additionally fitted the model using weighted regression (Supplementary Table 3, model 2(LS)). All analyses were performed using R v.3.3.2 (ref. 41). The hierarchical model (equations 4a–c) was fitted with INLA, using the R-interface R-INLA (version built on 20 June 2017), which can be downloaded from [www.r-inla.org](http://www.r-inla.org).

**Ethics statement.** This work complies with institutional guidelines and the guidelines for work with animals: Swiss animal experimentation permit no. GR\_6/2007.

**Reporting Summary.** Further information on research design is available in the Nature Research Reporting Summary linked to this article.

## Data availability

The data that support the findings of this study have been deposited in Dryad Digital Repository<sup>52</sup>.

Received: 21 March 2018; Accepted: 26 July 2019;  
Published online: 2 September 2019

## References

- Hedrick, P. W. & Garcia-Dorado, A. Understanding inbreeding depression, purging, and genetic rescue. *Trends Ecol. Evol.* **31**, 940–952 (2016).

2. Wallace, B. Hard and soft selection revisited. *Evolution* **29**, 465–473 (1975).
3. Agrawal, A. F. & Whitlock, M. C. Mutation load: the fitness of individuals in populations where deleterious alleles are abundant. *Annu. Rev. Ecol. Evol. Syst.* **43**, 115–135 (2012).
4. Johnson, H. E., Mills, L. S., Wehausen, J. D., Stephenson, T. R. & Luikart, G. Translating effects of inbreeding depression on component vital rates to overall population growth in endangered bighorn sheep. *Conserv. Biol.* **25**, 1240–1249 (2011).
5. Reed, T. E., Grotan, V., Jenouvrier, S., Saether, B.-E. & Visser, M. E. Population growth in a wild bird is buffered against phenological mismatch. *Science* **340**, 488–491 (2013).
6. Agrawal, A. F. & Whitlock, M. C. Environmental duress and epistasis: how does stress affect the strength of selection on new mutations? *Trends Ecol. Evol.* **25**, 450–458 (2010).
7. Creel, S. Recovery of the Florida panther—genetic rescue, demographic rescue, or both? Response to Pimm et al. (2006). *Anim. Conserv.* **9**, 125–126 (2006).
8. Wootton, J. T. & Pfister, C. A. Processes affecting extinction risk in the laboratory and in nature. *Proc. Natl Acad. Sci. USA* **112**, E5903 (2015).
9. Hufbauer, R. A. et al. Reply to Wootton and Pfister: the search for general context should include synthesis with laboratory model systems. *Proc. Natl Acad. Sci. USA* **112**, E5904– (2015).
10. Kardos, M., Taylor, H. R., Ellegren, H., Luikart, G. & Allendorf, F. W. Genomics advances the study of inbreeding depression in the wild. *Evol. Appl.* **9**, 1205–1218 (2016).
11. Stuwe, M. & Nievergelt, B. Recovery of Alpine ibex from near extinction: the result of effective protection, captive breeding, and reintroductions. *Appl. Anim. Behav. Sci.* **29**, 379–387 (1991).
12. Grotan, V., Saether, B. E., Filli, F. & Engen, S. Effects of climate on population fluctuations of ibex. *Glob. Change Biol.* **14**, 218–228 (2008).
13. Biebach, I. & Keller, L. F. A strong genetic footprint of the re-introduction history of Alpine ibex (*Capra ibex ibex*). *Mol. Ecol.* **18**, 5046–5058 (2009).
14. Biebach, I. & Keller, L. F. Genetic variation depends more on admixture than number of founders in reintroduced Alpine ibex populations. *Biol. Conserv.* **147**, 197–203 (2012).
15. Biebach, I. & Keller, L. F. D. Inbreeding in reintroduced populations: the effects of early reintroduction history and contemporary processes. *Conserv. Genet.* **11**, 527–538 (2010).
16. Crow, J. F. in *Statistics and Mathematics in Biology* (eds Kempthorne, O. et al.) 543–556 (Iowa State Univ. Press, 1954).
17. Jacquard, A. in *The Genetic Structure of Populations* (ed. Jacquard, A.) 160–219 (Springer, 1974).
18. Vitalis, R., Dawson, K. & Boursot, P. Interpretation of variation across marker loci as evidence of selection. *Genetics* **158**, 1811–1823 (2001).
19. Weir, B. S. & Goudet, J. A unified characterization of population structure and relatedness. *Genetics* **206**, 2085–2103 (2017).
20. Holsinger, K. E. & Weir, B. S. Genetics in geographically structured populations: defining, estimating and interpreting  $F_{ST}$ . *Nat. Rev. Genet.* **10**, 639–650 (2009).
21. Vitalis, R. & Couvet, D. Estimation of effective population size and migration rate from one- and two-locus identity measures. *Genetics* **157**, 911–925 (2001).
22. Fuller, W. A. *Measurement Error Models* (John Wiley & Sons, 1987).
23. Muff, S., Riebler, A., Held, L., Rue, H. & Saner, P. Bayesian analysis of measurement error models using integrated nested Laplace approximations. *J. R. Stat. Soc. Ser. C* **64**, 231–252 (2015).
24. Yun, L. & Agrawal, A. F. Variation in the strength of inbreeding depression across environments: effects of stress and density dependence. *Evolution* **68**, 3599–3606 (2014).
25. Gilpin, M. E. & Soulé, M. E. in *Conservation Biology, the Science of Scarcity and Diversity* (ed. Soulé, M. E.) 19–34 (Sinauer Associates, 1986).
26. Wright, S. Size of population and breeding structure in relation to evolution. *Science* **87**, 430–431 (1938).
27. Beaumont, M. A. Estimation of population growth or decline in genetically monitored populations. *Genetics* **164**, 1139–1160 (2003).
28. Facon, B. et al. Inbreeding depression is purged in the invasive insect *armonia axyridis*. *Curr. Biol.* **21**, 424–427 (2011).
29. Garcia-Dorado, A. Understanding and predicting the fitness decline of shrunk populations: inbreeding, purging, mutation, and standard selection. *Genetics* **190**, 1461–1476 (2012).
30. Glemin, S. How are deleterious mutations purged? Drift versus nonrandom mating. *Evolution* **57**, 2678–2687 (2003).
31. Kirkpatrick, M. & Jarne, P. The effects of a bottleneck on inbreeding depression and the genetic load. *Am. Nat.* **155**, 154–167 (2000).
32. Whiteley, A. R., Fitzpatrick, S. W., Funk, W. C. & Tallmon, D. A. Genetic rescue to the rescue. *Trends Ecol. Evol.* **30**, 42–49 (2015).
33. Saccheri, I. et al. Inbreeding and extinction in a butterfly metapopulation. *Nature* **392**, 491–494 (1998).
34. O'Grady, J. J. et al. Realistic levels of inbreeding depression strongly affect extinction risk in wild populations. *Biol. Conserv.* **133**, 42–51 (2006).
35. Goldberg, E. E. et al. Species selection maintains self-incompatibility. *Science* **330**, 493–495 (2010).
36. Nievergelt, B. *Der Alpensteinbock (Capra ibex L.) in Seinem Lebensraum* (Verlag Paul Parey, 1966).
37. Abderhalden, W. D. *Raumnutzung und Sexuelle Segregation* (Albert-Ludwigs-Universität Freiburg i. Brsg., 2004).
38. Saether, B. E., Lillegard, M., Grotan, V., Filli, F. & Engen, S. Predicting fluctuations of reintroduced ibex populations: the importance of density dependence, environmental stochasticity and uncertain population estimates. *J. Anim. Ecol.* **76**, 326–336 (2007).
39. Jaquiere, J., Guillaume, F. & Perrin, N. Predicting the deleterious effects of mutation load in fragmented populations. *Conserv. Biol.* **23**, 207–218 (2009).
40. Ciofi, C., Beaumont, M. A., Swingland, I. R. & Bruford, M. W. Genetic divergence and units for conservation in the Komodo dragon *Varanus komodoensis*. *Proc. R. Soc. Lond. B* **266**, 2269–2274 (1999).
41. R Development Core Team R: *A Language and Environment for Statistical Computing* (R Foundation for Statistical Computing, 2016); <http://www.R-project.org>
42. Grossen, C., Biebach, I., Angelone-Alasaad, S., Keller, L. F. & Croll, D. Population genomics analyses of European ibex species show lower diversity and higher inbreeding in reintroduced populations. *Evol. Appl.* **11**, 123–139 (2018).
43. Aeschbacher, A. *Das Brunnverhalten des Alpensteinwildes* (Rentsch, 1978).
44. Harvey, A. C. *Forecasting, Structural Time Series Models and the Kalman Filter* (Cambridge Univ. Press, 1989).
45. Schooler, S. S., Salau, B., Julien, M. H. & Ives, A. R. Alternative stable states explain unpredictable biological control of *Salvinia molesta* in Kakadu. *Nature* **470**, 86–89 (2011).
46. Dennis, B., Ponciano, J. M., Lele, S. R., Taper, M. L. & Staples, D. F. Estimating density dependence, process noise, and observation error. *Ecol. Monogr.* **76**, 323–341 (2006).
47. MathWorks MATLAB (The MathWorks, 2012).
48. Kendall, M. & Stuart, A. *The Advanced Theory of Statistics* Vol. 2 (Griffin, 1979).
49. Carroll, R., Ruppert, D., Stefanski, L. & Crainiceanu, C. *Measurement Error in Nonlinear Models: A Modern Perspective* (Chapman & Hall, 2006).
50. Rue, H., Martino, S. & Chopin, N. Approximate Bayesian inference for latent Gaussian models by using integrated nested Laplace approximations. *J. R. Stat. Soc. Ser. B* **71**, 319–392 (2009).
51. Spiegelhalter, D. J., Best, N. G., Carlin, B. R. & van der Linde, A. Bayesian measures of model complexity and fit. *J. R. Stat. Soc. Ser. B* **64**, 583–616 (2002).
52. Bozzuto, C., Biebach, I., Muff, S., Ives, A. R. & Keller, L. F. Inbreeding reduces long-term growth of Alpine ibex populations. *Dryad Digital Repository* <https://doi.org/10.5061/dryad.dc1s8h3> (2019).

## Acknowledgements

We thank the many people who helped us obtain genetic samples from Alpine ibex, especially the cantonal authorities and game wardens. We also thank the Swiss Federal Office for the Environment (FOEN) for the count and harvest data, and Wildtier Schweiz for access to their archives of ibex reintroduction history. We are grateful to S. Aeschbacher and B. Oberholzer for gathering information from these archives, and to T. Bucher and G. Camenisch for help in the laboratory. M. Beaumont provided important insights, and comments by J. Bascompte, E. Albert, H. Kokko, I. Saccheri and K. Strier improved the manuscript. The FOEN financially supported this project.

## Author contributions

I.B. and L.F.K. conceived and designed the study and collected the samples. I.B. performed the genetic analyses and compiled the demographic data. C.B. and A.R.I. analysed the time series data. S.M. performed the measurement-error modelling. All authors wrote the manuscript.

## Competing interests

The authors declare no competing interests.

## Additional information

**Supplementary information** is available for this paper at <https://doi.org/10.1038/s41559-019-0968-1>.

**Reprints and permissions information** is available at [www.nature.com/reprints](http://www.nature.com/reprints).

**Correspondence and requests for materials** should be addressed to A.R.I. or L.F.K.

**Publisher's note:** Springer Nature remains neutral with regard to jurisdictional claims in published maps and institutional affiliations.

© The Author(s), under exclusive licence to Springer Nature Limited 2019

## Reporting Summary

Nature Research wishes to improve the reproducibility of the work that we publish. This form provides structure for consistency and transparency in reporting. For further information on Nature Research policies, see [Authors & Referees](#) and the [Editorial Policy Checklist](#).

### Statistics

For all statistical analyses, confirm that the following items are present in the figure legend, table legend, main text, or Methods section.

n/a Confirmed

- The exact sample size ( $n$ ) for each experimental group/condition, given as a discrete number and unit of measurement
- A statement on whether measurements were taken from distinct samples or whether the same sample was measured repeatedly
- The statistical test(s) used AND whether they are one- or two-sided  
*Only common tests should be described solely by name; describe more complex techniques in the Methods section.*
- A description of all covariates tested
- A description of any assumptions or corrections, such as tests of normality and adjustment for multiple comparisons
- A full description of the statistical parameters including central tendency (e.g. means) or other basic estimates (e.g. regression coefficient) AND variation (e.g. standard deviation) or associated estimates of uncertainty (e.g. confidence intervals)
- For null hypothesis testing, the test statistic (e.g.  $F$ ,  $t$ ,  $r$ ) with confidence intervals, effect sizes, degrees of freedom and  $P$  value noted  
*Give  $P$  values as exact values whenever suitable.*
- For Bayesian analysis, information on the choice of priors and Markov chain Monte Carlo settings
- For hierarchical and complex designs, identification of the appropriate level for tests and full reporting of outcomes
- Estimates of effect sizes (e.g. Cohen's  $d$ , Pearson's  $r$ ), indicating how they were calculated

*Our web collection on [statistics for biologists](#) contains articles on many of the points above.*

### Software and code

Policy information about [availability of computer code](#)

Data collection

*Provide a description of all commercial, open source and custom code used to collect the data in this study, specifying the version used OR state that no software was used.*

Data analysis

We used the software 2mod to estimate population specific  $F_{st}$ , the software PLINK to estimate runs of homozygosity and various custom code written in R and Matlab. The custom R-code together with the data used for the regression analysis is available on Dryad (doi: 10.5061/dryad.dc1s8h3). Other code is available upon request.

For manuscripts utilizing custom algorithms or software that are central to the research but not yet described in published literature, software must be made available to editors/reviewers. We strongly encourage code deposition in a community repository (e.g. GitHub). See the Nature Research [guidelines for submitting code & software](#) for further information.

### Data

Policy information about [availability of data](#)

All manuscripts must include a [data availability statement](#). This statement should provide the following information, where applicable:

- Accession codes, unique identifiers, or web links for publicly available datasets
- A list of figures that have associated raw data
- A description of any restrictions on data availability

The time series and allele frequencies data that support the findings of this study in addition to the Supplementary Information are available on Dryad (doi: 10.5061/dryad.dc1s8h3).

## Field-specific reporting

Please select the one below that is the best fit for your research. If you are not sure, read the appropriate sections before making your selection.

Life sciences       Behavioural & social sciences       Ecological, evolutionary & environmental sciences

For a reference copy of the document with all sections, see [nature.com/documents/nr-reporting-summary-flat.pdf](https://www.nature.com/documents/nr-reporting-summary-flat.pdf)

## Life sciences study design

All studies must disclose on these points even when the disclosure is negative.

Sample size

Data exclusions

Replication

Randomization

Blinding

## Reporting for specific materials, systems and methods

We require information from authors about some types of materials, experimental systems and methods used in many studies. Here, indicate whether each material, system or method listed is relevant to your study. If you are not sure if a list item applies to your research, read the appropriate section before selecting a response.

### Materials & experimental systems

n/a	Involved in the study
<input type="checkbox"/>	<input type="checkbox"/> Antibodies
<input type="checkbox"/>	<input type="checkbox"/> Eukaryotic cell lines
<input type="checkbox"/>	<input type="checkbox"/> Palaeontology
<input type="checkbox"/>	<input type="checkbox"/> Animals and other organisms
<input type="checkbox"/>	<input type="checkbox"/> Human research participants
<input type="checkbox"/>	<input type="checkbox"/> Clinical data

### Methods

n/a	Involved in the study
<input type="checkbox"/>	<input type="checkbox"/> ChIP-seq
<input type="checkbox"/>	<input type="checkbox"/> Flow cytometry
<input type="checkbox"/>	<input type="checkbox"/> MRI-based neuroimaging

## Antibodies

Antibodies used

Validation

## Eukaryotic cell lines

Policy information about [cell lines](#)

Cell line source(s)

Authentication

Mycoplasma contamination

Commonly misidentified lines (See [ICLAC](#) register)

## Palaeontology

Specimen provenance



## Specimen deposition

Indicate where the specimens have been deposited to permit free access by other researchers.

## Dating methods

If new dates are provided, describe how they were obtained (e.g. collection, storage, sample pretreatment and measurement), where they were obtained (i.e. lab name), the calibration program and the protocol for quality assurance OR state that no new dates are provided.

Tick this box to confirm that the raw and calibrated dates are available in the paper or in Supplementary Information.

## Animals and other organisms

Policy information about [studies involving animals](#); [ARRIVE guidelines](#) recommended for reporting animal research

## Laboratory animals

For laboratory animals, report species, strain, sex and age OR state that the study did not involve laboratory animals.

## Wild animals

Provide details on animals observed in or captured in the field; report species, sex and age where possible. Describe how animals were caught and transported and what happened to captive animals after the study (if killed, explain why and describe method; if released, say where and when) OR state that the study did not involve wild animals.

## Field-collected samples

For laboratory work with field-collected samples, describe all relevant parameters such as housing, maintenance, temperature, photoperiod and end-of-experiment protocol OR state that the study did not involve samples collected from the field.

## Ethics oversight

Identify the organization(s) that approved or provided guidance on the study protocol, OR state that no ethical approval or guidance was required and explain why not.

Note that full information on the approval of the study protocol must also be provided in the manuscript.

## Human research participants

Policy information about [studies involving human research participants](#)

## Population characteristics

Describe the covariate-relevant population characteristics of the human research participants (e.g. age, gender, genotypic information, past and current diagnosis and treatment categories). If you filled out the behavioural & social sciences study design questions and have nothing to add here, write "See above."

## Recruitment

Describe how participants were recruited. Outline any potential self-selection bias or other biases that may be present and how these are likely to impact results.

## Ethics oversight

Identify the organization(s) that approved the study protocol.

Note that full information on the approval of the study protocol must also be provided in the manuscript.

## Clinical data

Policy information about [clinical studies](#)

All manuscripts should comply with the ICMJE [guidelines for publication of clinical research](#) and a completed [CONSORT checklist](#) must be included with all submissions.

## Clinical trial registration

Provide the trial registration number from [ClinicalTrials.gov](#) or an equivalent agency.

## Study protocol

Note where the full trial protocol can be accessed OR if not available, explain why.

## Data collection

Describe the settings and locales of data collection, noting the time periods of recruitment and data collection.

## Outcomes

Describe how you pre-defined primary and secondary outcome measures and how you assessed these measures.

## ChIP-seq

### Data deposition

Confirm that both raw and final processed data have been deposited in a public database such as [GEO](#).

Confirm that you have deposited or provided access to graph files (e.g. BED files) for the called peaks.

## Data access links

May remain private before publication.

For "Initial submission" or "Revised version" documents, provide reviewer access links. For your "Final submission" document, provide a link to the deposited data.

## Files in database submission

Provide a list of all files available in the database submission.

Genome browser session  
(e.g. [UCSC](#))

Provide a link to an anonymized genome browser session for "Initial submission" and "Revised version" documents only, to enable peer review. Write "no longer applicable" for "Final submission" documents.

## Methodology

Replicates	<i>Describe the experimental replicates, specifying number, type and replicate agreement.</i>
Sequencing depth	<i>Describe the sequencing depth for each experiment, providing the total number of reads, uniquely mapped reads, length of reads and whether they were paired- or single-end.</i>
Antibodies	<i>Describe the antibodies used for the ChIP-seq experiments; as applicable, provide supplier name, catalog number, clone name, and lot number.</i>
Peak calling parameters	<i>Specify the command line program and parameters used for read mapping and peak calling, including the ChIP, control and index files used.</i>
Data quality	<i>Describe the methods used to ensure data quality in full detail, including how many peaks are at FDR 5% and above 5-fold enrichment.</i>
Software	<i>Describe the software used to collect and analyze the ChIP-seq data. For custom code that has been deposited into a community repository, provide accession details.</i>

## Flow Cytometry

### Plots

Confirm that:

- The axis labels state the marker and fluorochrome used (e.g. CD4-FITC).
- The axis scales are clearly visible. Include numbers along axes only for bottom left plot of group (a 'group' is an analysis of identical markers).
- All plots are contour plots with outliers or pseudocolor plots.
- A numerical value for number of cells or percentage (with statistics) is provided.

### Methodology

Sample preparation	<i>Describe the sample preparation, detailing the biological source of the cells and any tissue processing steps used.</i>
Instrument	<i>Identify the instrument used for data collection, specifying make and model number.</i>
Software	<i>Describe the software used to collect and analyze the flow cytometry data. For custom code that has been deposited into a community repository, provide accession details.</i>
Cell population abundance	<i>Describe the abundance of the relevant cell populations within post-sort fractions, providing details on the purity of the samples and how it was determined.</i>
Gating strategy	<i>Describe the gating strategy used for all relevant experiments, specifying the preliminary FSC/SSC gates of the starting cell population, indicating where boundaries between "positive" and "negative" staining cell populations are defined.</i>

Tick this box to confirm that a figure exemplifying the gating strategy is provided in the Supplementary Information.

## Magnetic resonance imaging

### Experimental design

Design type	<i>Indicate task or resting state; event-related or block design.</i>
Design specifications	<i>Specify the number of blocks, trials or experimental units per session and/or subject, and specify the length of each trial or block (if trials are blocked) and interval between trials.</i>
Behavioral performance measures	<i>State number and/or type of variables recorded (e.g. correct button press, response time) and what statistics were used to establish that the subjects were performing the task as expected (e.g. mean, range, and/or standard deviation across subjects).</i>

## Acquisition

Imaging type(s)

Field strength

Sequence & imaging parameters

Area of acquisition

Diffusion MRI  Used  Not used

## Preprocessing

Preprocessing software

Normalization

Normalization template

Noise and artifact removal

Volume censoring

## Statistical modeling & inference

Model type and settings

Effect(s) tested

Specify type of analysis:  Whole brain  ROI-based  Both

Statistic type for inference (See [Eklund et al. 2016](#))

Correction

## Models & analysis

n/a | Involved in the study

Functional and/or effective connectivity

Graph analysis

Multivariate modeling or predictive analysis

Functional and/or effective connectivity

Graph analysis

Multivariate modeling and predictive analysis